A wide-band continuous-beam-scanning leaky-wave antenna with a stable gain fed by spoof surface plasmon polaritons

CHAI Bo[1]*, LI Yajing[2], and BAI Yukun[1]

1. *Engineering Research Center of Communication Devices and Technology, Ministry of Education, School of Integrated Circuit Science and Engineering, Tianjin University of Technology, Tianjin 300384, China*
2. *Shanghai University, Shanghai 200072, China*

(Received 27 August 2021; Revised 4 October 2021)

A leaky-wave antenna (LWA) supporting wide-band and continuous-beam scanning is proposed in this paper. It is based on a spoof surface plasmon polariton (SSPP) transmission line (TL) periodically loaded with circular patches. The optimized antenna structure enables its continuous-beam scanning of 69° from backward through broadside to forward with a stable high radiation gain as the operating frequency increases from 7 GHZ to 15 GHz (with a relative bandwidth of 72.73%). Furthermore, a perfect electronic conductor (PEC) reflector is added at a distance of about $0.3\lambda_0$ (λ_0 is the vacuum wavelength for the broadside radiation) to improve the antenna gain, achieving a gain increase of about 3 dB. The proposed LWA is expected to find applications in planar wireless communication systems.
Document code: A **Article ID:** 1673-1905(2022)04-0210-5
DOI https://doi.org/10.1007/s11801-022-1134-6

Leaky-wave antenna (LWA) is a travelling-wave antenna under intensive research, which can be used in many applications, such as frequency modulated continuous wave radar[1], real-time spectrum analysis[2], and field pattern synthesis[3], due to its ideal characteristics of high directivity, simple feed network[4] and frequency-following beam scanning[5]. However, conventional LWAs suffer from the broadside stopband effect, limited bandwidth and unconformability[6].

Surface plasmon polaritons (SPPs)[7] are surface waves which break the diffraction limit and are confined to the sub-wavelength region, resulting in conformable and miniature waveguides. It is expected to have potential applications in constructing integrated and miniaturized devices, such as filters, wave splitters, and antennas[8]. Conventionally, SPPs are in the infrared or visible frequency regime. To achieve similar characteristics in the microwave and terahertz frequency regimes[9], spoof surface plasmon polaritons (SSPPs) realized by excavating periodic grooves on a metal layer were proposed. Ref.[10] shows how to realize the dispersion relation similar to the SPPs by corrugating its surface with a periodic array of radial grooves. After that, it is found that the transmission characteristics of SSPPs are closely related to the geometry[11] of the metal layer and material properties[12] of the metal and dielectric in contact. The typical metal-layer configuration consists of different types of periodic grooves[13-16] slotted in the metal strip. A wide-band continuous single-beam scanning LWA based on an SSPPs transmission line (TL) loaded with circular patches on a single side was presented[13], in which the SSPPs-TL was realized by slotting rectangular holes in a metallic strip. In Ref.[14], a wide-scanning-angle circularly polarized LWA was reported. In Ref.[15], a novel LWA was proposed, which was realized by arranging periodic counterchanged sinusoidal structures on both sides of the SSPPs TL. In addition, ZHU et al[16] proposed a high efficiency and consistent gain LWA fed by planar SSPPs waveguide, in which the SSPPs waveguide was realized by introducing interdigital branches into metal strips. However, most of these designs have either relatively narrow bandwidth or large overall dimensions.

In this paper, a wide-band continuous beam scanning LWA based on an SSPPs TL is proposed, which is constructed by slotting a periodic trapezoidal structure in a metallic strip. The SSPPs waveguide is modulated by alternatively loading periodic circular patches on both sides of the SSPPs waveguide. The proposed SSPPs-LWA features a stable high gain over a wide bandwidth and continuous beam scanning.

The geometry of the proposed LWA excited by SSPPs waveguide is illustrated in Fig.1(a). The LWA was fabricated on a 1-mm-thick F4B dielectric substrate (ε_r=2.65, tanδ=0.003). Its overall size is $L\times W$=316 mm×55.56 mm. The structure consists of three parts, including coplanar

* E-mail: cb183127318@163.com

waveguides (CPW) and transition sections at two ends, and the modulated SSPPs waveguide in between. In this article, a method to improve the antenna radiation gain is proposed, which is to place a ground plate under the LWA, as shown in Fig.1(b). When the distance between the LWA and the ground plate is S_0=0.3, λ_0=9 mm, the radiation gain of the LWA is improved most significantly, where λ_0 is the space wavelength at 10 GHz.

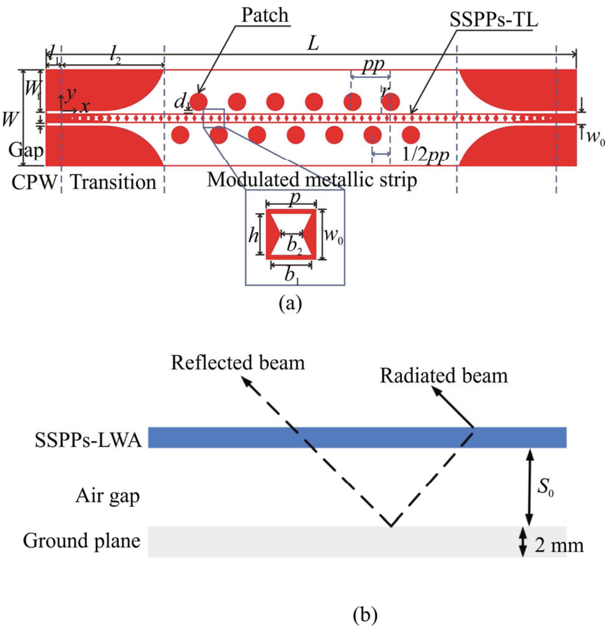

Fig.1 LWA: (a) Geometrical configuration; (b) Side view

The SSPPs unit cell is shown in the inset of Fig.1(a) with geometric parameters of p=5 mm, w_0=5 mm, h=4 mm, b_1=4 mm, b_2=2 mm, which ensures the TL characteristic impedance of 50 Ω. The SSPPs unit cell was analyzed by the Eigen-mode solver of CST Microwave Studio. As shown in Fig.2, the SSPPs have similar dispersion characteristics as SPPs. According to the dispersion curves in Fig.2(a), the cut-off frequency of the SSPPs mode is decreased as the groove depth h increases, hence the greater constraint of the surface wave to the waveguide, and Fig.2(b) shows that the width b_2 of the trapezoid has negligible effect on the dispersion characteristics. According to Fig.2(a), the cutoff frequency of the specified SSPPs unit cell is 17.15 GHz.

SSPPs-TL is a single conductor TL that supports TM surface electromagnetic waves. Due to its geometric symmetry, it is easy to be matched with the 50 Ω coax feed line through SMA connectors. Fig.3(a) and (b) show the simulated E_y electric field and H_z magnetic field of the TL at 10 GHz, respectively. We can clearly observe the laterally confined and alternately-distributed transverse fields between the two sides of the SSPPs waveguide. This allows metal patches to be placed on either side or both sides of the SSPPs waveguide to convert the guided SSPPs slow wave into radiated fast wave. S-parameters of the TL are shown in Fig.4, which indicate a wide bandwidth of 2—17 GHz for S_{11}<−10 dB. The wide bandwidth of the designed SSPPs waveguide is the basis for the wide bandwidth operation of the SSPPs-LWA.

As mentioned before, in order to efficiently transform the SSPPs guided wave into a radiation wave, we divide the LWA into three parts. The first part is the CPW, in which the TEM wave propagates, and its propagation constant is k_0. In order to achieve impedance matching at two ends, CPW is designed so that it has characteristic impedance of 50 Ω. The optimized dimensions of the CPW are w_0=5 mm, l_1=17 mm, and gap=0.28 mm. The second part is the transition section for mode conversion between TEM wave in the CPW and TM surface wave in the SSPPs waveguide. In other words, it enables the matching of wave vector and impedance between the two types of waveguides. The transition section consists of eight SSPPs unit cells with gradually increasing width and groove depth. The curve of the outer metal in the transition section is a quarter ellipse with a half long-axis length of l_2=60 mm and a half short-axis length of W_f=30 mm. The third part is the SSPPs waveguide loaded with periodic circular patches on both sides, where the SSPPs surface wave is coupled to the radiation wave.

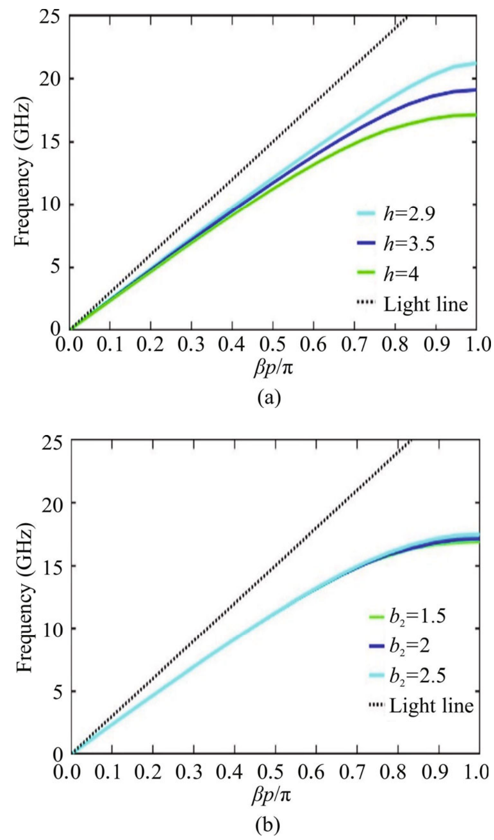

Fig.2 Dispersion curves of the SSPPs unit cell with (a) *p*=5 mm, w_0=5 mm, b_1=4 mm, b_2=2 mm for different *h* and (b) *p*=5 mm, w_0=5 mm, *h*=4 mm, b_1=4 mm for different b_2

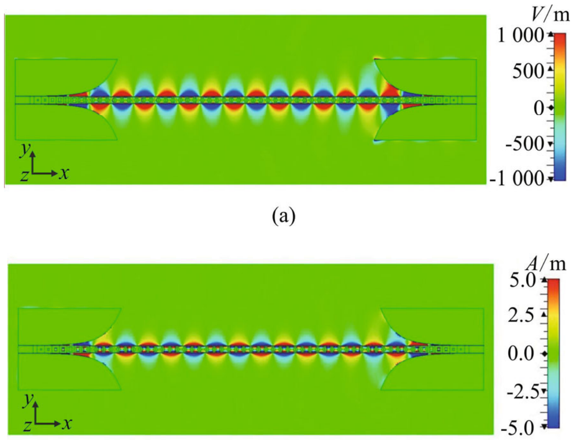

(a)

(b)

Fig.3 Simulated electric-field and magnetic-field distributions of the SSPPs waveguide at 10 GHz: (a) E_y-component; (b) H_z-component

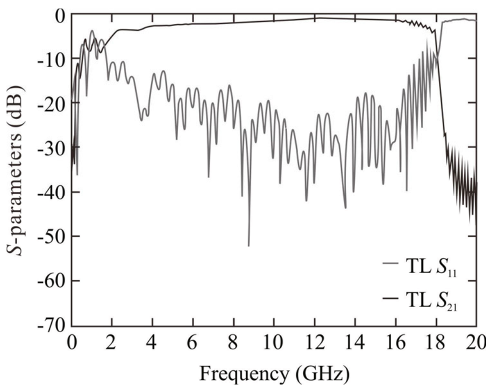

Fig.4 S-parameters of the SSPPs TL

Because SSPPs waveguide supports slow surface mode $k_{\mathrm{SSPPs}}>k_0$, SSPPs surface waves cannot radiate into free space. In order to achieve the purpose of radiation, periodic disturbances are introduced to stimulate higher order harmonics. According to the Floquet theory, the propagation constant of the n-th harmonic β_n satisfies

$$\beta_n=\beta_0+2\pi n/pp, n=0,\pm1,\pm2,\cdots, \tag{1}$$

where β_0 is the propagation constant of the SSPPs slow wave, and pp is the modulation period. Because it is ideal that only a single harmonic will form leaky-wave radiation, we normally use the space harmonic $n=-1$. Because β_{-1} can be negative or positive, the radiation beam of the LWA can be steered in either forward or backward direction. The main beam direction can be calculated from β_{-1} as

$$\theta=\arcsin(\beta_{-1}/k_0), \tag{2}$$

where k_0 is the wavenumber in free space.

The proposed LWA is designed to radiate in the broadside direction at 10 GHz. As shown in Fig.2(a), the SSPPs waveguide wavelength is $\lambda_g=2\pi/\beta=23$ mm at 10 GHz. From Eqs.(1) and (2), we conclude that in order to achieve a broadside radiation at 10 GHz, the loaded-patch period should be equal to the waveguide wavelength, i.e., $pp=\lambda_g=23$ mm. Through simulations, it is found that the position of the circular patch will affect the performance of the LWA. When the patch centers are placed at the location of the maximum magnetic fields, the performance of LWA will reach optimum. The distance t between the patch and the SSPPs-TL affects the coupling energy from the TL. The patch radius r and the distance t between the patch and the SSPPs waveguide are optimized to enhance the coupling level and hence the radiated power, and the optimized parameters are $r=\lambda_g/4=5.75$ mm and $d=1.5$ mm.

Compared with Fig.4, Fig.5 shows S_{21} of the LWAs is significantly reduced due to the leaky radiation from the antennas and the impedance bandwidth is also reduced. But the wide impedance bandwidth of the feeding SSPPs waveguide definitely leads to the wide bandwidth operation of the designed SSPPs-LWA. Fig.6 shows the phase distributions of the antenna at different frequencies. With the increase of frequency, the main beam shifts from the backward direction to the forward direction. In consistence with our design, the radiation is in the broadside direction at 10 GHz.

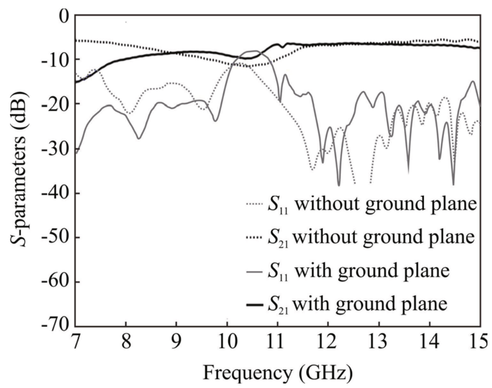

Fig.5 Simulated results of S-parameters with and without a ground plan

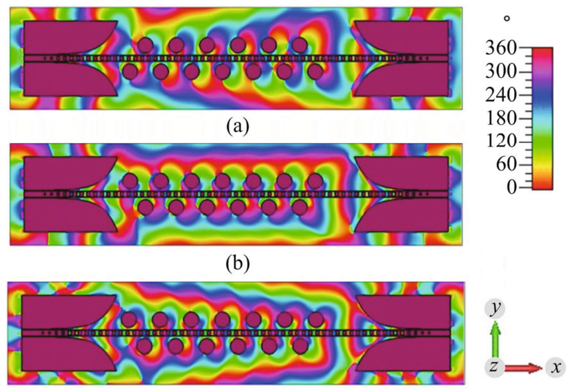

(a)

(b)

(c)

Fig.6 Phase distributions of the proposed SSPPs-LWA at different frequencies: (a) 9 GHz; (b) 10 GHz; (c) 11 GHz

Fig.7 shows 3D far-field radiation patterns of SSPPs-LWA. Antennas with and without ground plane have good consistency. Fig.8 presents the radiation gain and main beam angle with and without ground plane as frequency varies from 7 GHz to 15 GHz. It shows that the LWAs with and without a ground plane are in good agreement in both cases. In the whole bandwidth, the average radiation gain is 13.72 dBi and the beam scanning range is 69°. Therefore, a reasonably high and stable radiation gain is achieved in the bandwidth. The simulated radiation efficiency and total efficiency of the proposed antenna are shown in Fig.9. The antenna efficiencies with and without ground plane are also reasonably high and stable, with an average radiation efficiency of 82.23% and 83.65%, respectively.

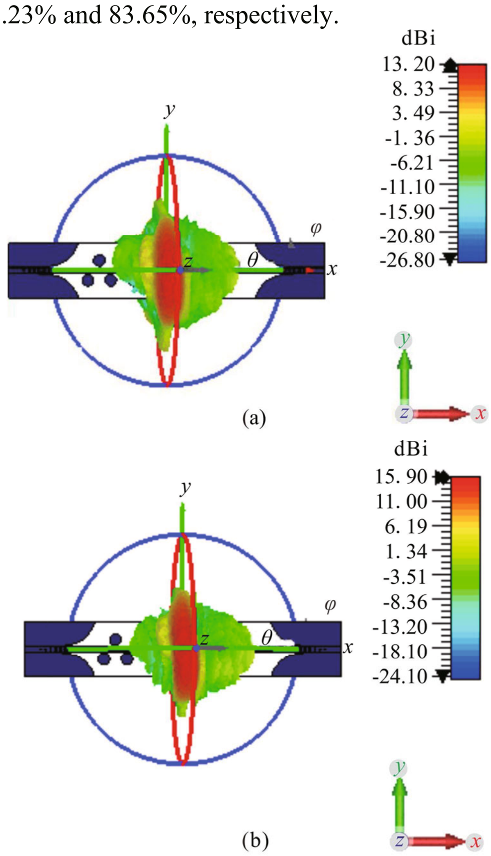

Fig.7 3D far-field radiation patterns of the LWA at 10 GHz: (a) Antenna without a ground plane; (b) Antenna with a ground plane

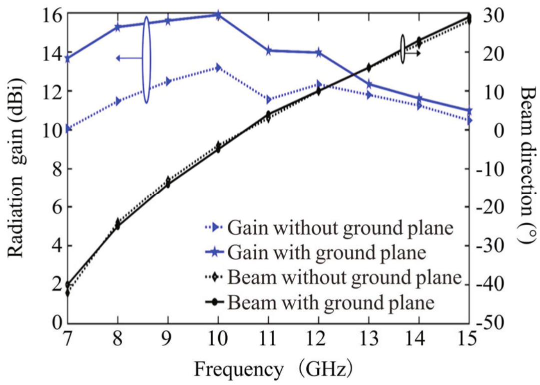

Fig.8 Radiation gain and main beam direction versus frequency

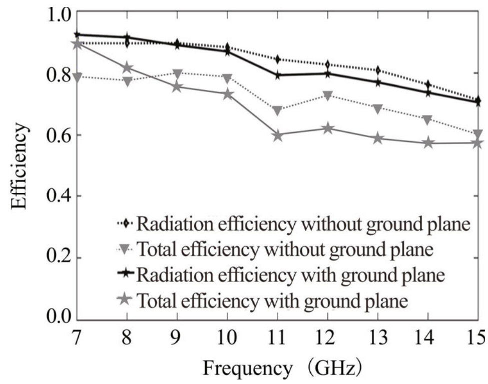

Fig.9 Simulated radiation and total efficiencies

To quantitatively show the advantages of the proposed antenna, we compare it with other SPPs-based LWAs in Tab.1. Note that the proposed LWA achieves rather good performance in terms of radiation gain and bandwidth.

Tab.1 Comparison with other SPPs-based LWA

Structure	Frequency (GHz)	Scanning range (°)	Average gain (dBi)
Ref.[13]	7—15 (72.73%)	65	12
Ref.[14]	4.5—7 (43.48%)	50	10
Ref.[15]	4—10 (85.71%)	110	9
Ref.[16]	11—16 (37.04%)	60	12
This work	7—15 (72.73%)	69	13.72

An LWA fed by an SSPPs waveguide has been proposed in this paper. Circular patches are periodically loaded on both sides of the SSPPs waveguide to convert the SSPPs slow wave into the space fast wave. The proposed antenna can continuously scan through the broadside with a scanning range of 69° as the operating frequency increases from 7 GHz to 15 GHz. Furthermore, a method is proposed to increase the radiation gain of the antenna by about 3 dB, and the LWA achieves a high and stable gain with an average value of about 13.72 dBi, and an average radiation efficiency of about 82.23%. In addition, the proposed SSPPs-LWA has a large bandwidth compared with previously reported counterparts. It has great potential to be applied in beam-scanning microwave wireless systems.

Statements and Declarations

The authors declare that there are no conflicts of interest related to this article.

References

[1] KAIVANTO E K, BERG M, SALONEN E, et al. Wearable circularly polarized antenna for personal satellite communication and navigation[J]. IEEE transactions on antennas propagation, 2011, 59(12): 4490-4496.

[2] HAO Z C, ZHANG J, ZHAO L. A compact leaky-wave antenna using a planar spoof surface plasmon polariton structure[J]. International journal of RF and micro-wave

computer-aided engineering, 2019, 29(5) : 21617-21623.

[3] CHEN H, MA H, LI Y, et al. Wideband frequency scanning spoof surface plasmon polariton planar antenna based on transmissive phase gradient metasurface[J]. IEEE antennas and wireless propagation letters, 2018, 17(3): 463-467.

[4] FAN Y, WANG J, LI Y, et al. Frequency scanning radiation by decoupling spoof surface plasmon polaritons via phase gradient metasurface[J]. IEEE antennas and wireless propagation letters, 2017, 17(1): 203-208.

[5] LIAO Z, ZHAO J, PAN B C, et al. Broadband transition between microstrip line and conformal surface plasmon waveguide[J]. Journal of physics D-applied physics, 2014, 47(31): 315103.

[6] PATEL A M, GRBIC A. A printed peaky-wave antenna based on a sinusoidally-modulated reactance surface[J]. IEEE transactions on antennas propagation, 2011, 59(6): 2087-2096.

[7] YIN J Y, REN J, ZHANG Q, et al. Frequency controlled broad-angle beam scanning of patch array fed by spoof surface plasmon polaritons[J]. IEEE transactions on antennas propagation, 2016, 64(12): 5181-5189.

[8] YI H, QU S W, BAI X, et al. Antenna array excited by spoof planar plasmonic waveguide[J]. IEEE transactions on antennas propagation, 2014, 13: 1227-1230.

[9] ZHANG Q L, ZHANG Q, CHEN Y. High-efficiency circularly polarised leaky-wave antenna fed by spoof surface plasmon polaritons[J]. IET microwaves antennas and propagation, 2018, 12(10): 1639-1644.

[10] JIA Y Y, CUI T J. Frequency-controlled beam scanning array fed by spoof surface plasmon polaritons[C]//2017 IEEE International Symposium on Antennas and Propagation and USNC/URSI National Radio Science Meeting, July 9-14, 2017, San Diego, CA, USA. New York: IEEE, 2017: 1271-1272.

[11] PORS A, MORENO E, MARTIN L, et al. Localized spoof plasmons arise while texturing closed surfaces[J]. Physical review letters, 2012, 108(22): 223905-223910.

[12] XU J J, JIANG X, ZHANG H C, et al. Diffraction radiation based on an anti-symmetry structure of spoof surface-plasmon waveguide[J]. Applied physics letters, 2017, 110(2): 021118-021122.

[13] LIU L, CHEN M, CAI J, et al. Single beam leaky wave antenna with lateral continuous scanning functionality based on spoof surface plasmon transmission line[J]. IEEE access, 2019, 7: 25225-25231.

[14] BAI Y K, CHENG A F. A spoof surface plasmon leaky wave antenna with circular polarization[J]. International journal of RF and microwave computer-aided engineering, 2020, 30(8): 22248-22254.

[15] ZHONG T, ZHANG H. Spoof surface plasmon polaritons excited leaky-wave antenna with continuous scanning range from endfire to forward[J]. Chinese physics B, 2020, 29(09): 369-374.

[16] ZHU A Q, LIAO X, WANG B, et al. Compact spoof surface plasmon polariton leaky wave antenna with consistent cain[J]. Microwave and optical technology letters, 2021, 63(9): 2430-2435.